Available online at www.sciencedirect.com
ScienceDirect
Journal of Approximation Theory 163 (2011) 1349–1372
JOURNAL OF Approximation Theory
www.elsevier.com/locate/jat

Full length article

Set-valued Hermite interpolation☆

Robert Baier*, Gilbert Perria

University of Bayreuth, Chair of Applied Mathematics, 95440 Bayreuth, Germany

Received 23 November 2009; received in revised form 18 June 2010; accepted 12 November 2010
Available online 8 March 2011

Communicated by Nira Dyn

Abstract

The problem of interpolating a set-valued function with convex images is addressed by means of directed sets. A directed set will be visualised as a usually non-convex set in $\mathbb{R}^n$ consisting of three parts together with its normal directions: the convex, the concave and the mixed-type part. In the Banach space of the directed sets, a mapping resembling the Kergin map is established. The interpolating property and error estimates similar to the point-wise case are then shown; the representation of the interpolant through means of divided differences is given. A comparison to other set-valued approaches is presented. The method developed within the article is extended to the scope of the Hermite interpolation by using the derivative notion in the Banach space of directed sets. Finally, a numerical analysis of the explained technique corroborates the theoretical results.

Keywords: Set-valued interpolation; Hermite interpolation; Embedding of convex, compact sets; Directed sets; Derivatives of set-valued maps

1. Introduction

Hermite interpolation is still a matter of recent research. To mention a few examples, it is applied in the following fields: the construction of shape preserving interpolation methods with C^1- or C^2-functions (cf. [28]); the interpolation of Bézier curves and patches (cf. [27]);

☆ This work was partially supported by the Hausdorff Research Institute for Mathematics, Bonn, within the HIM Junior Semester Program "Computational Mathematics" in February–April 2008.
* Corresponding author.
E-mail addresses: robert.baier@uni-bayreuth.de (R. Baier), gilbert.perria@googlemail.com (G. Perria).

0021-9045/$ - see front matter
doi:10.1016/j.jat.2010.11.004

terrain modelling and reconstruction as in [22]; the analysis of subdivision schemes incorporating derivative data as in [16]; the interpolation of α-level sets for fuzzy sets (cf. [19]). Another field of application is the analysis of linear/nonlinear partial differential equations. Here, the Hermite interpolant, as a function of x for fixed time t, has given function and derivative values of a regular solution $y(\cdot, t)$ of the PDE (cf. [20,7]). More applications and references are listed in the preprint [6].

The main difficulties in extending the notation and algorithms to the set-valued case (even in the simplest setting of $\mathcal{C}(\mathbb{R}^n)$, the set of convex compact non-empty subsets of $\mathbb{R}^n$) arise when defining a suitable difference and a suitable derivative. Known approaches like the geometric difference as in [21] or the Demyanov difference as in [11] carry the disadvantage of generating either too small (even empty) or too big (convex) sets. In any case, the set $\mathcal{C}(\mathbb{R}^n)$ is not a vector space.

To overcome these difficulties, embeddings as proposed by Rådström, Hörmander can be used. The main disadvantage is the lack of a visualisation of differences of embedded convex sets as subsets of $\mathbb{R}^n$. For more references and a detailed discussion, cf. [32,2].

Directed sets are the n-dimensional generalisation of generalised/directed intervals (cf. [24]) and provide an embedding of $\mathcal{C}(\mathbb{R}^n)$ into the Banach space $\overrightarrow{\mathcal{D}}^n$ of the directed sets. The embedding admits generalisations of the known set arithmetics like the Minkowski addition and multiplication with non-negative scalars; it also delivers a visualisation for differences of embedded sets from $\mathcal{C}(\mathbb{R}^n)$, cf. [2,3]. Directed sets were successfully applied to calculate and visualise the approximation and derivatives of set-valued maps in [4] and to polynomial Lagrange interpolation in [33]. For these reasons, the focus lies on the embedding by directed sets.

In this paper, the work [33] is extended to Hermite interpolation. Some of the results achieved in [36,14,34,17,39] for polynomial interpolation in Banach spaces can be applied, since $\overrightarrow{\mathcal{D}}^n$ is itself a Banach space. These pioneering works were aimed at more theoretical results, whereas here we focus on the numerical analysis; in fact, error estimates are not provided in [36] or demand in [34,17,39] too much regularity. We shall point out that, although the regularity assumptions in [14] are rather weak, the conditions (i), (ii), H1 in [14] for deriving error estimates (in $\overrightarrow{\mathcal{D}}^n$) still demand research. Furthermore, no numerical results of set-valued interpolation are visualised in these works unlike in [26,33].

We will present simple recursive proofs as well as a representation through means of two components (a lower-dimensional directed set together with a scalar function); in this way, connections to other approaches as in [26] are revealed easier than with arguments in [33] based on Banach spaces (cf. Section 5). Therein, polynomial interpolation with higher degree than one may generate negative weights; the interpolating polynomial of the support function is then no longer convex with respect to the direction and additional geometric assumptions have therefore to be posed to ensure the non-emptiness of the sets.

The directed sets, which constitute the main tool within this work, will be introduced in Section 2. Therein, the embedding J_n in [2] from the cone of the convex compact subsets of $\mathbb{R}^n$ into $\overrightarrow{\mathcal{D}}^n$ is recalled. The section following is intended to acquaint the reader with a notion for differentiability of *convex-valued* set-valued maps, i.e. with the notion of *directed differentiability*. There, the notations for the divided differences and polynomial interpolation as well as basic facts are recalled and specialised to the directed sets. The *Hermite–Genocchi* formula and an estimate for divided differences and the remainder term of the interpolating polynomial are presented. Continuing, the interpolating map $\mathcal{K}_\Theta F$ is introduced in Section 4 and some remainder formulae are illustrated which generalise well-known error estimates to the

set-valued case. Piecewise Hermite interpolation of sets and error estimates for the derivatives of the interpolant are studied as well. Finally, the numerical results are gathered in the last section, showing that the directed sets are indeed a convenient tool for performing Hermite interpolation.

2. Directed sets

2.1. Preliminaries

In this introductory subsection, the notation will be fixed and basic definitions will be presented.

Denote by $\|\cdot\|$ the Euclidean norm in $\mathbb{R}^n$, let $B_r(m)$ be the corresponding closed ball in $\mathbb{R}^n$ with radius r and centre $m \in \mathbb{R}^n$ and $S_{n-1} \subset \mathbb{R}^n$ the unit sphere. The class of all non-empty convex compact sets in $\mathbb{R}^n$ is called $\mathcal{C}(\mathbb{R}^n)$. The support function $\delta^*(\cdot, A)$ of a set $A \in \mathcal{C}(\mathbb{R}^n)$ is defined in $\mathbb{R}^n$ as

$$\delta^*(l, A) := \max_{a \in A} \langle l, a \rangle. \tag{1}$$

We leave out intentionally a review of the properties of the support function (cf. [37,38]) assuming these to be well-known to the reader.

For any $l \in \mathbb{R}^n$ and $A \in \mathcal{C}(\mathbb{R}^n)$, we denote with

$$Y(l, A) = \left\{ a \in A \mid \langle l, a \rangle = \delta^*(l, A) \right\} \tag{2}$$

the *supporting face* of A in the direction l. It equals the subdifferential $\partial \delta^*(l, A)$ of the support function. An element from $Y(l, A)$ will be denoted by $y(l, A)$ or, alternatively, in the more compact fashion y_A^l.

We consider the usual arithmetic operations, i.e. the *Minkowski addition*

$$A + B := \{a + b \mid a \in A, b \in B\} \tag{3}$$

for $A, B \in \mathcal{C}(\mathbb{R}^n)$ and the multiplication by a real scalar $\lambda \in \mathbb{R}$

$$\lambda \cdot A := \{\lambda \cdot a \mid a \in A\}$$

(cf. e.g. [13]). For the particular case as for $\lambda = -1$, the notation $\ominus A$ is also often used. The *geometric/Pontryagin's difference* in [21] is defined as

$$A \stackrel{*}{-} B := \bigcap_{l \in S_{n-1}} \left\{ x \in \mathbb{R}^n \mid \langle l, x \rangle \leq \delta^*(l, A) - \delta^*(l, B) \right\}$$

which might be empty.

We denote by $\mathrm{d_H}(A, B)$ the *Hausdorff distance* of the two sets and by $\mathrm{d_D}(A, B)$ the corresponding *Demyanov distance*; cf. [11] for the original definition of the Demyanov distance and [33, Proposition 2.4.5].

2.2. Definition of directed sets

At this stage, basic facts concerning the directed sets introduced in [2,3] are briefly recalled. A directed set $\overrightarrow{A}$ is parameterised by directions $l \in S_{n-1}$ and consists of two components: a continuous function $a_n(l)$ and a $(n-1)$-dimensional uniformly bounded directed set function, $\overrightarrow{A_{n-1}(l)}$.

Let $a(\cdot)$ be a function from S_{n-1} into $\mathbb{R}$, $l \in S_{n-1}$ and

$$\mathcal{H}_a^l := \left\{x \in \mathbb{R}^n \mid \langle l, x\rangle = a(l)\right\} \tag{4}$$

denote the corresponding hyperplane. $\mathcal{H}_a^l$ and $\mathbb{R}^{n-1}$ being isomorph for each $l \in S_{n-1}$, we introduce the affine function (shortly called *projection*)

$$\Pi_a^l : \mathcal{H}_a^l \longrightarrow \mathbb{R}^{n-1} \tag{5}$$

whose corresponding linear function is the isomorphic projection from $\mathcal{H}_0^l$ onto $\mathbb{R}^{n-1}$ (cf. [2,4]). The above function generates an (affine) *re-projection*

$${}^*\Pi_a^l : \mathbb{R}^{n-1} \longrightarrow \mathcal{H}_a^l \tag{6}$$

with $(\Pi_a^l \circ {}^*\Pi_a^l)(x) = x$ for all $x \in \mathcal{H}_a^l$.

For a directed set, the hyperplane $\mathcal{H}_a^l$ is fixed by $a(l) = a_n(l)$.

A directed set is defined recursively with respect to its dimension $n \in \mathbb{N}$.

Definition 1. Consider $n \in \mathbb{N}$ and denote with $\overrightarrow{\mathcal{D}}^n$ the space of the directed sets of dimension n. A directed set of dimension $\mathbf{n} = \mathbf{1}$ is given by the expression

$$\overrightarrow{A} := (a_1(l))_{l\in S_0} = (a_1(-1), a_1(+1))$$

for a function $a_1(\cdot) : S_0 \longrightarrow \mathbb{R}$. The norm of the one-dimensional $\overrightarrow{A}$ is given as

$$\|\overrightarrow{A}\|_1 := \max_{l\in S_0} |a_1(l)| = \max\{|a_1(-1)|, |a_1(+1)|\}.$$

For higher dimensions $\mathbf{n} \geq \mathbf{2}$, a directed set $\overrightarrow{A} \in \overrightarrow{\mathcal{D}}^n$ is defined by a function

$$\begin{aligned} &\overrightarrow{A} : S_{n-1} \longrightarrow \overrightarrow{\mathcal{D}}^{n-1} \times \mathbb{R} \\ &l \mapsto (\overrightarrow{A_{n-1}(l)}, a_n(l)). \end{aligned}$$

Here, the second component $a_n(\cdot) : S_{n-1} \to \mathbb{R}$ is continuous and the first component $\overrightarrow{A_{n-1}(\cdot)} : S_{n-1} \to \overrightarrow{\mathcal{D}}^{n-1}$ has to be uniformly bounded with regard to the norm $\|\cdot\|_{n-1}$. The norm in $\overrightarrow{\mathcal{D}}^n$ is defined recursively as

$$\|\overrightarrow{A}\|_n := \max\{\sup_{l\in S_{n-1}} \|\overrightarrow{A_{n-1}(l)}\|_{n-1}, \max_{l\in S_{n-1}} |a_n(l)|\}. \tag{7}$$

We remark that for denoting a directed set $\overrightarrow{A} \in \overrightarrow{\mathcal{D}}^n$ the compact form

$$\left(\overrightarrow{A}_{n-1}^l, a_n^l\right)_{l\in S_{n-1}} \tag{8}$$

will be also often used. Notice that for $n = 1$ only the right-hand component is to be considered. Moreover, when the dimension n appears clear from the context, we drop the subscript in (7).

Convex compact sets can be embedded into the Banach space of the directed sets; of course, the embedding is also recursively defined. For further references on other possible embeddings and related articles see [2,3].

Definition 2. The embedding $J_n : \mathcal{C}(\mathbb{R}^n) \longrightarrow \overrightarrow{\mathcal{D}}^n$ is given by

$$J_n(A) = \begin{cases} (\delta^*(l, A))_{l\in S_0} & \text{for } n = 1, \\ (J_{n-1}(\Pi^l_{\delta^*(\cdot,A)}(Y(l, A))), \delta^*(l, A))_{l\in S_{n-1}} & \text{for } n \geq 2. \end{cases}$$

From the definition above, we gather that, for an embedded convex compact set C, the hyperplane $\mathcal{H}^l_{a_n}$ as in (4) is determined by the value of its support function $\delta^*(\cdot, C)$ in direction l, whereas $\overrightarrow{A_{n-1}(l)}$ is the embedded projection of its supporting face $Y(l, C)$ (seen as $(n-1)$-dimensional set) into $\overrightarrow{\mathcal{D}}^{n-1}$.

The operations of a real vector space are introduced component-wise in $\overrightarrow{\mathcal{D}}^n$.

Definition 3. For $\overrightarrow{A} = (\overrightarrow{A}^l_{n-1}, a^l_n)_{l\in S_{n-1}}$, $\overrightarrow{B} = (\overrightarrow{B}^l_{n-1}, b^l_n)_{l\in S_{n-1}} \in \overrightarrow{\mathcal{D}}^n$ and $\lambda, \mu \in \mathbb{R}$, the operations are defined recursively:

$$\lambda \cdot \overrightarrow{A} + \mu \cdot \overrightarrow{B} := (\lambda \cdot \overrightarrow{A}^l_{n-1} + \mu \cdot \overrightarrow{B}^l_{n-1}, \lambda\, a^l_n + \mu\, b^l_n)_{l\in S_{n-1}}.$$

Notice that the first component of a directed set is not present for $n = 1$.

2.3. Properties of directed sets

Endowed with the above operations, the space $\overrightarrow{\mathcal{D}}^n$ enjoys remarkable properties which are portrayed in [2]. Above all, $\overrightarrow{\mathcal{D}}^n$ is a Banach space (see [2, Theorem 3.9]). Since we are basically interested in embedded elements of $\mathcal{C}(\mathbb{R}^n)$ (along with their difference and visualisation), we restrict our attention to the Banach space consisting of the closure of the linear hull $\overrightarrow{\mathcal{C}}^n$ of $J_n(\mathcal{C}(\mathbb{R}^n))$ with respect to the norm in Definition 1.

The embedding in Definition 2 commutes with the addition, therefore preserving the Minkowski-sum, as well as with the multiplication with a non-negative scalar as shown in [2, Theorem 4.17].

Proposition 1. *Let A and B be in $\mathcal{C}(\mathbb{R}^n)$. Furthermore, consider real scalars $\lambda \geq 0$ and $\mu \geq 0$. Then the following equality holds:*

$$J_n(\lambda \cdot A + \mu \cdot B) = \lambda \cdot J_n(A) + \mu \cdot J_n(B).$$

We now recall basic notion concerning the visualisation of directed sets; for more details, the reader may refer to [3]. The visualisation of a directed set $\overrightarrow{A} \in \overrightarrow{\mathcal{C}}^n$ consists of three parts: the *convex part*

$$P_n(\overrightarrow{A}) := \bigcap_{l\in S_{n-1}} \left\{x \in \mathbb{R}^n \mid \langle l, x\rangle \leq a_n(l)\right\}, \tag{9}$$

the *concave part*

$$N_n(\overrightarrow{A}) := \ominus \bigcap_{l\in S_{n-1}} \left\{x \in \mathbb{R}^n \mid \langle l, x\rangle \leq -a_n(l)\right\}, \tag{10}$$

and the (non-convex) *mixed-type part*

$$M_n(\overrightarrow{A}) := B_n(\overrightarrow{A}) \setminus (\partial P_n(\overrightarrow{A}) \cup \partial N_n(\overrightarrow{A})). \tag{11}$$

Here, $B_n(\overrightarrow{A})$ is the *boundary part* given by

$$B_n(\overrightarrow{A}) := \begin{cases} \partial P_1(\overrightarrow{A}) \cup \partial N_1(\overrightarrow{A}) = \{-a_1(-1), a_1(+1)\}, & \text{if } n = 1, \\ \bigcup\limits_{l \in S_{n-1}} {}^*\Pi^l_{a_n}(V_{n-1}(\overrightarrow{A_{n-1}(l)})), & \text{if } n \geq 2. \end{cases} \tag{12}$$

The *visualisation* is defined as the union

$$V_n(\overrightarrow{A}) := P_n(\overrightarrow{A}) \cup N_n(\overrightarrow{A}) \cup M_n(\overrightarrow{A}). \tag{13}$$

For each boundary point $x \in B_n(\overrightarrow{A})$, the *orientation bundle* denotes a set of unit directions with

$$\mathcal{O}_1(x, \overrightarrow{A}) := \begin{cases} \{-1\}, & \text{if } \overrightarrow{A} = \pm J_1([a,b]),\ a < b \text{ and } x = \pm a, \\ \{+1\}, & \text{if } \overrightarrow{A} = \pm J_1([a,b]),\ a < b \text{ and } x = \pm b, \\ \{\pm 1\}, & \text{if } \overrightarrow{A} = J_1(\{a\}), \qquad a = b \text{ and } x = a, \end{cases} \tag{14}$$

$$\mathcal{O}_n(x, \overrightarrow{A}) := \{l \in S_{n-1} : x \in {}^*\Pi^l_{a_n}(V_{n-1}(\overrightarrow{A_{n-1}(l)}))\}, \quad \text{if } n \geq 2. \tag{15}$$

It appears clear from the above definitions that the re-projection of the visualisation of $\overrightarrow{A_{n-1}(l)}$ lies on the hyperplane $\mathcal{H}^l_a$ (recall (4)). This image forms the boundary part of the visualised $\overrightarrow{A}$ in direction $l \in S_{n-1}$.

Remark 1. At this stage some useful properties of the visualisation should be mentioned; for a description of the mixed-type part we refer to [3]. First of all, the visualisation of an embedded convex set $\overrightarrow{A}$ equals the set itself, i.e.

$$V_n(\overrightarrow{A}) = P_n(\overrightarrow{A}) \equiv A, \qquad B_n(\overrightarrow{A}) = \partial A, \qquad M_n(\overrightarrow{A}) = \emptyset, \tag{16}$$

whereas for its inverse $-\overrightarrow{A}$ each boundary point of $\overrightarrow{A}$ is inverted, but preserves its orientation bundle, i.e.

$$\begin{aligned} &V_n(-\overrightarrow{A}) = \ominus V_n(\overrightarrow{A}), \qquad B_n(-\overrightarrow{A}) = \ominus B_n(\overrightarrow{A}), \\ &P_n(-\overrightarrow{A}) = \ominus N_n(\overrightarrow{A}), \qquad N_n(-\overrightarrow{A}) = \ominus P_n(\overrightarrow{A}), \qquad M_n(-\overrightarrow{A}) = \ominus M_n(\overrightarrow{A}) \end{aligned}$$

and $\mathcal{O}_n(-x, -\overrightarrow{A}) = \mathcal{O}_n(x, \overrightarrow{A})$ for all $x \in B_n(\overrightarrow{A})$.

Furthermore, the difference of two embedded sets $\overrightarrow{A}, \overrightarrow{B} \in \mathcal{C}(\mathbb{R}^n)$

$$P_n(\overrightarrow{A} - \overrightarrow{B}) = A \stackrel{*}{-} B, \qquad N_n(\overrightarrow{A} - \overrightarrow{B}) = \ominus(B \stackrel{*}{-} A)$$

includes the geometric difference in its visualisation. Finally, the visualisation and the boundary part of a general directed set is always non-empty: either the convex or concave part are non-empty (except for the degenerate case of a point) or, if both are empty, the mixed-type part is non-empty (see [3, Proposition 3.4]).

3. Set-valued derivatives and divided differences

The images of convex-valued set-valued maps defined on $I = [t_0, T] \subset \mathbb{R}$ are embedded into the Banach space $\overrightarrow{\mathcal{D}}^n$. Thus, the embedded function $\overrightarrow{F}$ is given by the composition $\overrightarrow{F} := J_n \circ F$ for a set-valued map $F : I \Rightarrow \mathbb{R}^n$ with convex images.

The usual notion of differentiability of functions having values in Banach spaces will be applied to embedded convex-valued maps as in [4].

Definition 4. A function $\overrightarrow{F} : I \to \overrightarrow{\mathcal{D}}^n$ is differentiable in $t \in I$, if the following limit exists:

$$\mathrm{D}\overrightarrow{F}(t) := \lim_{\substack{h\to 0\\ t+h\in I}} \frac{\overrightarrow{F}(t+h) - \overrightarrow{F}(t)}{h}. \tag{17}$$

The directed set $\mathrm{D}\overrightarrow{F}(t)$ is called the derivative of $\overrightarrow{F}$ at t. The derivatives $\mathrm{D}^k\overrightarrow{F}$ of higher order $k \geq 2$ are defined recursively in the usual way. A convex-valued function $F : I \Rightarrow \mathbb{R}^n$ is said to be directed differentiable in t, if its embedding $\overrightarrow{F} := J_n \circ F$ is differentiable in this point.

With the notation

$$\overrightarrow{F}(t) = (\overrightarrow{F}^{\,l}_{n-1}(t),\, f_n^l(t))_{l\in S_{n-1}} \tag{18}$$

resembling (8), we state the differentiability formula for the components of a directed set function. The norm in Definition 1 demands intrinsically a certain uniformity within the limit (17) with respect to the parameter $l \in S_{n-1}$.

Proposition 2. *If the map $\overrightarrow{F} : I \longrightarrow \overrightarrow{\mathcal{D}}^n$ is differentiable in $t \in I$, then both components are differentiable in t uniformly in $l \in S_{n-1}$ with the representation*

$$D\overrightarrow{F}(t) = (D\overrightarrow{F}^{\,l}_{n-1}(t),\, D f_n^l(t))_{l\in S_{n-1}}. \tag{19}$$

Proof. Recalling Definition 4 of the directed derivative, the limit

$$\lim_{\substack{h\to 0\\ t+h\in I}} \left(\frac{\overrightarrow{F}^{\,l}_{n-1}(t+h) - \overrightarrow{F}^{\,l}_{n-1}(t)}{h},\, \frac{f_n^l(t+h) - f_n^l(t)}{h} \right)_{l\in S_{n-1}} \tag{20}$$

forces the uniformity of the convergence for both components due to the definition of the norm (7), i.e. the assertion follows immediately. □

From the proposition above, we understand that the uniformly differentiability of both components implies the directed differentiability of the map $\overrightarrow{F}$. We now present a central criterion for the directed differentiability of a convex-valued function (refer to [33, Theorem 3.2.2]) that depends only on the differentiability of the support function of the supporting face.

Proposition 3 (*Characterisation of Smoothness*)**.** *The convex-valued map $F(\cdot)$ is directed differentiable in $t \in I$ if and only if the support function $\delta^*(\eta, Y(l, F(\cdot)))$ is differentiable in t uniformly in both arguments l and $\eta \in S_{n-1}$.*

Directed differentiability implies the smoothness of $t \mapsto \delta^*(l, F(t))$ uniformly in $l \in S_{n-1}$ which is very natural in the study of numerical methods for set-valued quadrature methods, in the study of set-valued Runge–Kutta methods and in set-valued interpolation (cf. [15,5,26] and references therein).

Corollary 1. *Suppose the convex-valued map $F(\cdot)$ to be directed differentiable in $t \in I$. Then, the support function $\delta^*(l, F(\cdot))$ is differentiable in t in the classical sense uniformly in $l \in S_{n-1}$.*

Proof. Being $\delta^*(l, Y(l, F(\cdot))) = \delta^*(l, F(\cdot))$, Proposition 3 can be applied. □

In the following, let $I = [t_0, T]$ be a compact interval with $t_0 < T$. By convention, $\Theta = (\theta_0, \ldots, \theta_k)$ will denote a *k-grid* on I of $k+1$ points $\theta_i \in I$, $i = 0, \ldots, k, k \in \mathbb{N}_0$, and $\Theta^j = (\theta_0, \ldots, \theta_j)$ the sub-grid of the first $j+1$ elements of Θ. co(Θ) will denote the convex hull of $\{\theta_0, \ldots, \theta_k\}$.

For any map $\overrightarrow{F} : \mathbb{R} \to \overrightarrow{\mathcal{D}}^n$, its divided difference of order j with respect to the k-grid Θ with distinct nodes θ_i, $i = 0, \ldots, k$, is recursively defined in the usual manner (see e.g. [9]) as in the following equations

$$\overrightarrow{F}[\theta_i] := \overrightarrow{F}(\theta_i), \tag{21}$$

$$\overrightarrow{F}[\theta_i, \theta_{i+1}, \ldots, \theta_{i+j}] := \frac{\overrightarrow{F}[\theta_{i+1}, \ldots, \theta_{i+j}] - \overrightarrow{F}[\theta_i, \ldots, \theta_{i+j-1}]}{\theta_{i+j} - \theta_i} \tag{22}$$

for $i = 0, \ldots, k-j$ in (21)–(22) with $j = 0$ in (21) resp. $j = 1, \ldots, k$ in (22).

The following lemma is meant to highlight, in the spirit of (18), the component-wise representation of the divided differences defined in (21)–(22).

Lemma 1. *Let $\overrightarrow{F} : I \to \overrightarrow{\mathcal{D}}^n$ and Θ be a k-grid on I of distinct points. Then, the divided difference $\overrightarrow{F}[\Theta]$ has the following component-wise representation:*

$$\overrightarrow{F}[\Theta] = (\overrightarrow{F}^l_{n-1}[\Theta],\ f^l_n[\Theta])_{l \in S_{n-1}}.$$

Proof. We proceed per induction on the order j of the divided difference.

For $j = 0$ and $i = 0, \ldots, k$, (21) yields trivially:

$$\overrightarrow{F}[\theta_i] = \overrightarrow{F}(\theta_i) = (\overrightarrow{F}^l_{n-1}(\theta_i),\ f^l_n(\theta_i))_{l \in S_{n-1}} = (\overrightarrow{F}^l_{n-1}[\Theta],\ f^l_n[\Theta])_{l \in S_{n-1}}. \tag{23}$$

For $j \geq 1$ and $i = 0, \ldots, k-j$, the recursive setting (22) applied to the j-grid $(\theta_i, \theta_{i+1}, \ldots, \theta_{i+j})$ can be rewritten as

$$\overrightarrow{F}[\theta_i, \theta_{i+1}, \ldots, \theta_{i+j}] = \frac{\overrightarrow{F}[\theta_{i+1}, \theta_{i+2}, \ldots, \theta_{i+j}] - \overrightarrow{F}[\theta_i, \theta_{i+1}, \ldots, \theta_{i+j-1}]}{\theta_{i+j} - \theta_i}.$$

The inductive hypothesis and the component-wise operations in $\overrightarrow{\mathcal{D}}^n$ finally yield

$$\begin{aligned}\overrightarrow{F}[\theta_i, \theta_{i+1}, \ldots, \theta_{i+j}] &= \frac{\left(\overrightarrow{F}^l_{n-1}[\theta_{i+1}, \theta_{i+2}, \ldots, \theta_{i+j}],\ f^l_n[\theta_{i+1}, \theta_{i+2}, \ldots, \theta_{i+j}]\right)_{l \in S_{n-1}}}{\theta_{i+j} - \theta_i} \\ &\quad - \frac{\left(\overrightarrow{F}^l_{n-1}[\theta_i, \theta_{i+1}, \ldots, \theta_{i+j-1}],\ f^l_n[\theta_i, \theta_{i+1}, \ldots, \theta_{i+j-1}]\right)_{l \in S_{n-1}}}{\theta_{i+j} - \theta_i} \\ &= \left(\overrightarrow{F}^l_{n-1}[\theta_i, \theta_{i+1}, \ldots, \theta_{i+j}],\ f^l_n[\theta_i, \theta_{i+1}, \ldots, \theta_{i+j}]\right)_{l \in S_{n-1}}. \quad \square\end{aligned}$$

The limiting process, i.e. collapsing nodes in the k-grid of the interpolation data, is studied in the next proposition. It guarantees a continuity property of the divided differences generalising the real-valued result, e.g. in [12].

Proposition 4. *Assume* $\overrightarrow{F} : I \longrightarrow \overrightarrow{\mathcal{D}}^n$ *to be k-times continuously differentiable at* $\theta \in I$. *Furthermore, assume that the nodes* $\theta_i, i = 0, \ldots, k$, *from the k-grids* Θ *in the following limit are all different. Then:*

$$\lim_{\substack{\theta_i \to \theta \\ 0 \le i \le k}} \overrightarrow{F}[\Theta] = \frac{1}{k!} \cdot D^k \overrightarrow{F}(\theta). \tag{24}$$

Moreover, for any $\varepsilon > 0$ *there exists a* $\delta = \delta(\varepsilon) > 0$ *depending on the continuity modulus of* $D^k \overrightarrow{F}(\cdot)$ *such that for all k-grids* Θ *with distinct nodes* θ_i, $i = 0, \ldots, k$, *and* $|\theta_i - \theta| \le \delta$ *it follows that*

$$\left\| \overrightarrow{F}[\Theta] - \frac{1}{k!} \cdot D^k \overrightarrow{F}(\theta) \right\| \le \varepsilon. \tag{25}$$

Proof. We shall proceed by induction on n.

For $n = 1$, Proposition 2 shows that $f_1^l(\cdot)$ is k-times continuously differentiable in θ uniformly in $l \in S_{n-1}$. Since this function is real-valued, we already know that

$$\lim_{\substack{\theta_i \to \theta \\ 0 \le i \le k}} f_1^l[\Theta] = \frac{1}{k!} \cdot \frac{\mathrm{d}^k}{\mathrm{d}t^k} f_1^l(\theta).$$

Additionally, for each $l \in S_0$ there exists $\xi^l \in \mathrm{co}\{\theta_0, \ldots, \theta_k\}$ with

$$f_1^l[\Theta] = \frac{1}{k!} \cdot \frac{\mathrm{d}^k}{\mathrm{d}t^k} f_1^l(\xi^l).$$

Since the k-th derivative of $\overrightarrow{F}(\cdot)$ is continuous, there exists $\delta = \delta(D^k \overrightarrow{F}) > 0$ such that for all $\theta_i \in [\theta - \delta, \theta + \delta] \cap I$, it follows that

$$\left| \frac{\mathrm{d}^k}{\mathrm{d}t^k} f_1^l(\xi^l) - \frac{\mathrm{d}^k}{\mathrm{d}t^k} f_1^l(\theta) \right| \le \| D^k \overrightarrow{F}(\xi^l) - D^k \overrightarrow{F}(\theta) \| \le k! \cdot \varepsilon, \tag{26}$$

because ξ^l is a convex combination of two nodes from Θ; δ depends only on $k! \cdot \varepsilon$ and on the continuity modulus of $D^k \overrightarrow{F}(\cdot)$.

Now, let $n \ge 2$. Proposition 2 shows that $f_n^l(\cdot)$ and $\overrightarrow{F}^l{}_{n-1}(\cdot)$ are k-times continuously differentiable in θ uniformly in $l \in S_{n-1}$. Because of the inductive assumption and the fact that $f_n^l(\cdot)$ is real-valued, it follows that

$$\lim_{\substack{\theta_i \to \theta \\ 0 \le i \le k}} \overrightarrow{F}^l{}_{n-1}[\Theta] = \frac{1}{k!} \cdot D^k \overrightarrow{F}^l{}_{n-1}(\theta) \quad \text{and} \quad \lim_{\substack{\theta_i \to \theta \\ 0 \le i \le k}} f_n^l[\Theta] = \frac{1}{k!} \cdot \frac{\mathrm{d}^k}{\mathrm{d}t^k} f_n^l(\theta).$$

The uniformity (with respect to $l \in S_{n-1}$) of the limits above is not yet evident. Moreover, the choice of $\delta(D^k \overrightarrow{F}^l{}_{n-1})$ in (26) seems to depend on the continuity modulus of each function $D^k \overrightarrow{F}^l{}_{n-1}(\cdot)$. Since

$$\begin{aligned} &\max \left\{ \| D^k \overrightarrow{F}^l{}_{n-1}(\theta_i) - D^k \overrightarrow{F}^l{}_{n-1}(\theta) \|, \left| \frac{\mathrm{d}^k}{\mathrm{d}t^k} f_n^l(\theta_i) - \frac{\mathrm{d}^k}{\mathrm{d}t^k} f_n^l(\theta) \right| \right\} \\ &\quad \le \| D^k \overrightarrow{F}(\theta_i) - D^k \overrightarrow{F}(\theta) \|, \end{aligned}$$

the inductive assumption can be exploited, $\delta(D^k \overrightarrow{F}^l_{n-1})$ depends only on $k! \cdot \varepsilon$ and on the continuity modulus of $D^k \overrightarrow{F}(\cdot)$ for each $l \in S_{n-1}$. For the second component function, that is real-valued, we can proceed as for $n = 1$; in fact, the argument with the continuity modulus can be repeated also here. Hence, the convergence is indeed uniformly in $l \in S_{n-1}$. Finally,

$$\begin{aligned}\lim_{\substack{\theta_i \to \theta \\ 0 \le i \le k}} \overrightarrow{F}[\Theta] &= \left(\lim_{\substack{\theta_i \to \theta \\ 0 \le i \le k}} \overrightarrow{F}^l_{n-1}[\Theta], \lim_{\substack{\theta_i \to \theta \\ 0 \le i \le k}} f^l_n[\Theta] \right)_{l \in S_{n-1}} \\ &= \left(\frac{1}{k!} \cdot D^k \overrightarrow{F}^l_{n-1}(\theta), \frac{1}{k!} \cdot \frac{\mathrm{d}^k}{\mathrm{d}t^k} f^l_n(\theta) \right)_{l \in S_{n-1}} = \frac{1}{k!} \cdot D^k \overrightarrow{F}(\theta). \quad \square\end{aligned}$$

Following [40, Section 2.1.3] and [12, Lemma 7.11 and subsequent remarks] we shall now extend the recursive formula (21)–(22) to the case of (some) coinciding points using the continuity as in Proposition 4. Let us assume that $\theta_i \le \theta_{i+1} \le \cdots \le \theta_{i+j}$. This involves no loss of generality because the divided difference are symmetric function of their arguments (cf. [17, Proposition 5.4], [40, (2.1.3.6) and Theorem (2.1.3.9)]). The recurrence relation will obviously fail in the case $\theta_{i+j} = \theta_i$ which also implies that $\theta_i = \theta_{i+1} = \cdots = \theta_{i+j}$. Applying (24), we thus distinguish the following two cases:

$$\overrightarrow{F}[\theta_i, \theta_{i+1}, \ldots, \theta_{i+j}] := \begin{cases} \dfrac{\overrightarrow{F}[\theta_{i+1}, \ldots, \theta_{i+j}] - \overrightarrow{F}[\theta_i, \ldots, \theta_{i+j-1}]}{\theta_{i+j} - \theta_i} & \text{if } \theta_{i+j} \ne \theta_i, \\ \dfrac{1}{j!} D^j \overrightarrow{F}(\theta_i) & \text{if } \theta_{i+j} = \theta_i. \end{cases} \tag{27}$$

We state a result concerning alternative representations of the divided differences. In the case of a general k-grid with (some) coinciding points one has the equivalence between the recursive definition given in (27) and a representation through means of a Bochner integral over the unit simplex.

Theorem 1. *Let $\Theta = (\theta_0, \ldots, \theta_k)$ be a general k-grid on I and $T_k \subset \mathbb{R}^k$ be the unit simplex. If $\overrightarrow{F} : I \to \overrightarrow{\mathcal{D}}^n$ is k-times continuously directed differentiable, then*

$$\overrightarrow{F}[\Theta] = \int_{T_k} \mathrm{D}^k \overrightarrow{F} \left(\theta_0 + \sum_{j=1}^{k} \nu_j (\theta_j - \theta_0) \right) \mathrm{d}\nu_1 \ldots \mathrm{d}\nu_k. \tag{28}$$

Proof. Cf. [17, Section 1]. $\square$

An equivalent formulation of the Hermite–Genocchi Formula in (28) based on a certain normalised spline is given by

$$\overrightarrow{F}[\Theta] = \frac{1}{k!} \int_I \mathrm{M}(t|\Theta) \mathrm{D}^k \overrightarrow{F}(t) \mathrm{d}t. \tag{29}$$

It is proved for directed sets in [33, Theorem 4.3.2] for distinct points. The function $\mathrm{M}(\cdot|\Theta)$ is the normalised B-spline with knots Θ and

$$\int_I \mathrm{M}(t|\Theta) \mathrm{d}t = 1 \tag{30}$$

(see e.g. [10] or [35]). An extensive treatment of B-splines and their properties can be found e.g. in [35, Sections 5.4 and 5.9] or [10, Chapter IX]. Evidently, the support of the spline $\mathrm{M}(\cdot|\Theta)$ is included in the convex hull $\mathrm{co}(\Theta)$. For (some) coinciding points, $\mathrm{M}(\cdot|\Theta)$ acts as a distribution, see [30] and [18, (4.4)].

Moreover, the integral on the right-hand in (28) and (29) are Bochner integrals, as introduced in [8], because the integrands take values in the Banach space $\overrightarrow{\mathcal{D}}^n$.

Thanks to Theorem 1, it is possible under certain assumptions, to derive immediately some useful properties of divided differences, in particular: the independence from the ordering of the knots in Θ; its continuity with respect to Θ; its meaning for collapsing points. For further details, one may see [34,17].

Proposition 5. *Let $\overrightarrow{F} : I \to \overrightarrow{\mathcal{D}}^n$ be the embedding of the convex-valued map $F : I \Rightarrow \mathbb{R}^n$ and Θ be a k-grid on I. If F is k-times continuously directed differentiable on I, then the estimate for the k-th divided difference is given by*

$$\|\overrightarrow{F}[\Theta]\| \leq \frac{1}{k!} \cdot \sup_{\theta \in [\theta_0, \theta_k]} \|D^k \overrightarrow{F}(\theta)\|. \tag{31}$$

Proof. The statement follows immediately from the Hermite–Genocchi formula (Theorem 1), the estimation of the Bochner integral by the norm of the integrand and from the fact that the volume of the unit simplex is $\frac{1}{k!}$. □

Another way to prove the estimate on the divided differences would be an induction on the space dimension n. For $n = 1$, the statement is well-known for real-valued functions; for $n \geq 2$, Lemma 1 allows you to study the two component functions separately. The argument for the second component is the same as for $n = 1$, the inductive assumption helps for the first component.

The main idea in the proof of [33, Theorem 4.3.2] consists in applying an induction per k (the order of the divided difference) and, based on (29), in using the recurrence formula for the derivative of the B-spline $N_j^k(\cdot)$ (cf. [10, Chapter IX]) involved in the definition of $M(\cdot|\Theta)$ to establish the statement. In [14,17] a different idea for the proofs has been pursued instead. Basically, the scalarisation, through means of functionals, of the functions taking their values in Banach spaces allows to apply well-known results for real-valued functions; finally, the separation of points by functionals is exploited to finish the proofs. In [34] the restriction to finite-dimensional subspaces containing interpolation points plays a major role.

At this stage all tools for introducing an interpolating map are established as for the real-valued case.

4. The (Kergin) interpolating map

We deliberately make use of the term "Kergin interpolation" and its notation to suggest that the presented approach may easily be extended to the scope of multivariate interpolation, see [30].

The following convention is introduced. Suppose that among the $k+1$ points $\theta_0, \ldots, \theta_k \in I = [t_0, T]$ only $m+1$, say $\widehat{\theta}_0, \ldots, \widehat{\theta}_m$, are distinct. Let θ_i occur in the list of points $\mu_i \geq 1$ times so that $k := \sum_{i=0}^m \mu_i - 1$, i.e.

$$\Theta := (\theta_0, \theta_1, \ldots, \theta_k) := \left(\underbrace{\widehat{\theta}_0, \ldots, \widehat{\theta}_0}_{\mu_0}, \ldots, \underbrace{\widehat{\theta}_i, \ldots, \widehat{\theta}_i}_{\mu_i}, \ldots, \underbrace{\widehat{\theta}_m, \ldots, \widehat{\theta}_m}_{\mu_m} \right). \tag{32}$$

Then, the (Hermite) interpolating map (denoted by $\mathcal{K}_\Theta \overrightarrow{F}$) for a $(\mu-1)$-times differentiable function $\overrightarrow{F} : I \to \overrightarrow{\mathcal{D}}^n$ with $\mu := \max_{i=0,\dots,m} \mu_i$ determines the (Hermite) polynomial map, for which the following interpolation conditions hold:

$$D^i(\mathcal{K}_\Theta \overrightarrow{F})(\widehat{\theta}_j) = D^i \overrightarrow{F}(\widehat{\theta}_j) \quad (i = 0, \dots, \mu_j - 1,\ j = 0, \dots, m). \tag{33}$$

The interpolation property in the following proposition is well-known (cf. [36, Theorems 4.3 and 5.2], [14], [34, Theorem 1], and [17, Theorem 5.7]) and generalises, cf. [12, Theorem 7.6], to the set-valued case. Hereby, the interpolation approach propagates to the components of the directed set function so that the interpolating map is always polynomial with respect to t.

Proposition 6. *Let Θ be the k-grid on I as in (32) and $\overrightarrow{F} : I \longrightarrow \overrightarrow{\mathcal{D}}^n$ be $(\mu-1)$-times continuously differentiable in I with $\mu := \max_{i=0,\dots,m} \mu_i$. Then, the polynomial map $\mathcal{K}_\Theta \overrightarrow{F} : I \to \overrightarrow{\mathcal{D}}^n$ of degree less or equal to k interpolating F on the k-grid Θ with conditions (33), is given by*

$$(\mathcal{K}_\Theta \overrightarrow{F})(t) := \sum_{j=0}^{k} \omega_\Theta^{j-1}(t) \cdot \overrightarrow{F}[\Theta^j]. \tag{34}$$

Hereby, $\omega_\Theta^{j-1}(t) = \prod_{i=0}^{j-1}(t-\theta_i)$, $j = 0, \dots, k$. The map above exhibits the following component-wise representation:

$$\mathcal{K}_\Theta \overrightarrow{F} \equiv (\mathcal{K}_\Theta \overrightarrow{F}^l{}_{n-1}, \mathcal{K}_\Theta f_n^l)_{l \in S_{n-1}}. \tag{35}$$

Proof. Set $\overrightarrow{H}(t) := \mathcal{K}_\Theta \overrightarrow{F}(t)$. First of all, Lemma 1 shows that

$$\overrightarrow{H}^l{}_{n-1}(t) = \sum_{j=0}^{k} \omega_\Theta^{j-1}(t) \cdot \overrightarrow{F}^l{}_{n-1}[\Theta^j], \qquad h_n^l(t) = \sum_{j=0}^{k} \omega_\Theta^{j-1}(t) \cdot f_n^l[\Theta^j]. \tag{36}$$

Proposition 2 allows to rewrite the interpolation conditions in (33) as

$$D^i(\overrightarrow{H}^l{}_{n-1})(\widehat{\theta}_j) = D^i \overrightarrow{F}^l{}_{n-1}(\widehat{\theta}_j), \qquad \frac{\mathrm{d}^i}{\mathrm{d}t^i} h_n^l(\widehat{\theta}_j) = \frac{\mathrm{d}^i}{\mathrm{d}t^i} f_n^l(\widehat{\theta}_j) \quad (i = 0, \dots, m_j - 1)$$

for $j = 0, \dots, m$. At this stage we proceed per induction on n.

$n = 1$: The uniqueness result for real-valued Hermite interpolation shows that $h_1^l = K_\Theta f_1^l$.

Similarly, for $n \geq 2$ one may immediately show that $h_n^l = K_\Theta f_n^l$. The inductive assumption shows that $\overrightarrow{H}^l{}_{n-1} = \mathcal{K}_\Theta \overrightarrow{F}^l{}_{n-1}$ and (35) follows from (36). □

The term $\mathcal{K}_\Theta \overrightarrow{F}$ respectively $\mathcal{K}_\Theta \overrightarrow{F}^l{}_{n-1}$ is the Kergin interpolating map in a Banach space (i.e. $\overrightarrow{\mathcal{D}}^n$ respectively $\overrightarrow{\mathcal{D}}^{n-1}$; refer to [34,17]); $\mathcal{K}_\Theta f_n^l$ is the well-known real-valued (Kergin) interpolating map (see e.g. [25]). The map in (34) is a polynomial with values in a Banach space in the sense of [36, Section 2], [14, Definition 2] and [17, Section 2].

After having introduced an interpolating map, we focus on deriving estimates for the interpolation error. We will denote with $\overrightarrow{\mathcal{R}_\Theta} := \overrightarrow{F} - \mathcal{K}_\Theta \overrightarrow{F}$ the remainder term; it acts

component-wise due to Proposition 6. For $l \in S_{n-1}$ we have

$$\begin{aligned} &\overrightarrow{\mathcal{R}}_\Theta = \left(\overrightarrow{\mathcal{R}}^l_{\Theta,n-1}, r^l_{\Theta,n}\right)_{l\in S_{n-1}}, \\ &\overrightarrow{\mathcal{R}}^l_{\Theta,n-1} = \overrightarrow{F}^l_{n-1} - \mathcal{K}_\Theta \overrightarrow{F}^l_{n-1}, \quad r^l_{\Theta,n} = f^l_n - \mathcal{K}_\Theta f^l_n. \end{aligned} \tag{37}$$

Variants of the following Proposition 7 are known. The error representation presented in (39) is proved in [17, Theorem 6.1] and used in [17, Theorem 6.2] to show an error estimate for the more restrictive class of holomorphic functions. For an estimation with the modulus of smoothness for Lagrange interpolation and for another embedding of $\mathcal{C}(\mathbb{R}^n)$ into a vector space under weaker smoothness assumptions, see [14, Corollary 3].

Proposition 7. *Let $\overrightarrow{F} : I \longrightarrow \overrightarrow{\mathcal{D}}^n$ be $(k+1)$-times continuously differentiable and $k = \left(\sum_{j=0}^m \mu_j\right) - 1$. Then the following error estimate holds for $t \in I$:*

$$\|\overrightarrow{\mathcal{R}}_\Theta(t)\| \le \frac{1}{(k+1)!} \cdot \|D^{k+1}\overrightarrow{F}\|_\infty \cdot \prod_{j=0}^m |t-\widehat{\theta}_j|^{\mu_j}. \tag{38}$$

Proof. With $\overrightarrow{\mathcal{R}}_\Theta$ as in (37) one has as in [34, Lemma 2]:

$$\overrightarrow{\mathcal{R}}_\Theta(t) = \omega^k_{(\Theta,t)}(t) \cdot \overrightarrow{F}[(\Theta,t)], \qquad \omega^k_{(\Theta,t)}(t) = \prod_{j=0}^m (t-\widehat{\theta}_j)^{\mu_j}. \tag{39}$$

Proposition 5 yields the assertion. □

The next two results are generalisations of the real-valued case. Other error estimates known for real-valued functions could be transferred to $\overrightarrow{\mathcal{D}}^n$ in a similar manner. The first estimation (cf. [23, Satz 3] for the real-valued case) provides an estimate for the interpolation error of the derivatives up to order $k+1$.

Lemma 2. *Let $\overrightarrow{F} : I \longrightarrow \overrightarrow{\mathcal{D}}^n$ be $(k+1)$-times continuously differentiable. Then, the following error estimate holds for $j = 0, \ldots, k+1$ and $t \in I$:*

$$\|D^j\overrightarrow{F}(t) - D^j(\mathcal{K}_\Theta\overrightarrow{F})(t)\| \le \frac{1}{(k+1-j)!} \cdot \|D^{k+1}\overrightarrow{F}\|_\infty \cdot \prod_{i=0}^{k-j} \max\{|t-\theta_i|, |t-\theta_{i+j}|\}.$$

Proof. We shall start with $n \ge 2$, since the real-valued case is known for $n = 1$, and set $\overrightarrow{H}(t) := \mathcal{K}_\Theta\overrightarrow{F}(t)$.

The second component of $\overrightarrow{F} - \overrightarrow{H}$ is estimated by [23, Satz 3] yielding

$$\begin{aligned} &\left|\frac{\mathrm{d}^j}{\mathrm{d}t^j} f^l_n(t) - \frac{\mathrm{d}^j}{\mathrm{d}t^j} h^l_n(t)\right| \\ &\quad \le \frac{1}{(k+1-j)!} \cdot \left\|\frac{\mathrm{d}^{k+1}}{\mathrm{d}t^{k+1}} f^l_n\right\|_\infty \cdot \prod_{i=0}^{k-j} \max\{|t-\theta_i|, |t-\theta_{i+j}|\}, \end{aligned} \tag{40}$$

where $j = 0, \dots, k+1$ and $l \in S_{n-1}$. Concerning the first component, one obtains with the inductive assumption:

$$\|D^j \overrightarrow{F}^l_{n-1}(t) - D^j \overrightarrow{H}^l_{n-1}(t)\| \leq \frac{1}{(k+1-j)!} \cdot \|D^{k+1} \overrightarrow{F}^l_{n-1}\|_\infty \cdot \prod_{i=0}^{k-j} \max\{|t-\theta_i|, |t-\theta_{i+j}|\}. \tag{41}$$

Since the estimates (40)–(41) and

$$\max\left\{ \|D^{k+1} \overrightarrow{F}^l_{n-1}\|_\infty, \left\| \frac{\mathrm{d}^{k+1}}{\mathrm{d}t^{k+1}} f_n^l \right\|_\infty \right\} \leq \|D^{k+1} \overrightarrow{F}\|_\infty$$

hold, the assertion follows. □

Consider a fixed step-size $h = \frac{T-t_0}{N}$, $N \in \mathbb{N}$, and the knot-grid $\widehat{\theta}_i := t_0 + ih \in I = [t_0, T]$, $i = 0, \dots, N$. Set

$$\Theta_i := \left(\underbrace{\widehat{\theta}_i, \dots, \widehat{\theta}_i}_{\mu}, \underbrace{\widehat{\theta}_{i+1}, \dots, \widehat{\theta}_{i+1}}_{\mu} \right),$$

$I_i := [\widehat{\theta}_i, \widehat{\theta}_{i+1}]$ and denote with $\overrightarrow{H}$ the piecewise defined map consisting of Hermite interpolating maps $\overrightarrow{H}_i$ on I_i for $i = 0, \dots, N$ with polynomial order $2\mu - 1$, $\mu_0 = \mu_1 = \mu$; thus: $m = 1$, $k = 2\mu - 1$ in (32) and

$$\mathcal{K}_{\Theta_i} \overrightarrow{F}\,|_{I_i} = \overrightarrow{H}_i.$$

Following the idea in the proof of [7, Theorem 2], we formulate the following estimation for the set-valued piecewise Hermite interpolation.

Corollary 2. *Assume $\overrightarrow{F} : I \to \overrightarrow{\mathcal{D}}^n$ to be (2μ)-times continuously differentiable. Then, the following error estimate holds for the piecewise Hermite interpolation with polynomial order $2\mu - 1$ and step-size h defined above for $t \in I$ and derivatives of order $j = 0, \dots, \mu - 1$:*

$$\|D^j \overrightarrow{F}(t) - D^j \overrightarrow{H}(t)\| \leq \frac{1}{(2\mu - j)!} \cdot \|D^{2\mu} \overrightarrow{F}\|_\infty \cdot h^{2\mu - j}. \tag{42}$$

Proof. Lemma 2 can be applied on I_i for $j = 0, \dots, 2\mu$ yielding

$$\begin{aligned} \|D^j \overrightarrow{F}(t) - D^j \overrightarrow{H}(t)\| &= \|D^j \overrightarrow{F}(t) - D^j \overrightarrow{H}_i(t)\| \\ &\leq \frac{1}{(2\mu - j)!} \cdot \|D^{2\mu} \overrightarrow{F}\|_\infty \cdot \prod_{\nu=0}^{2\mu-j-1} \max\{|t - \theta_{i,\nu}|, |t - \theta_{i,\nu+j}|\} \\ &\leq \frac{1}{(2\mu - j)!} \cdot \|D^{2\mu} \overrightarrow{F}\|_\infty \cdot h^{2\mu - j}, \end{aligned}$$

where $\theta_{i,\nu} = \widehat{\theta}_i$ for $\nu = 0, \dots, \mu - 1$ and $\theta_{i,\nu} = \widehat{\theta}_{i+1}$ for $\nu = \mu, \dots, 2\mu - 1$.

Notice that $\overrightarrow{H}$ is $(\mu - 1)$-times continuously differentiable on I, having the following conditions to hold for $i = 0, \dots, N-1$:

$$D^j \overrightarrow{H}(\widehat{\theta}_i) = D^j \overrightarrow{F}(\widehat{\theta}_i) \quad \text{and} \quad D^j \overrightarrow{H}(\widehat{\theta}_{i+1}) = D^j \overrightarrow{F}(\widehat{\theta}_{i+1}) \quad (j = 0, \dots, \mu - 1).$$

Hence, the global estimation on I is valid only for $j = 0, \dots, \mu - 1$. □

5. Connections to other approaches

Consider $t \in I$ and the representation of the images of a convex-valued map $F : I \Longrightarrow \mathbb{R}^n$ through means of the support function:

$$F(t) = \bigcap_{l \in S_{n-1}} \left\{ x \in \mathbb{R}^n \mid \langle l, x \rangle \leq \delta^l(t) \right\}. \tag{43}$$

Hereby, we set $\delta^l(t) := \delta^*(l, F(t))$ for simpleness of notation.

In [26], polynomial interpolation of δ^l for every $l \in S_{n-1}$ underlies the following set-valued approximation of $F(t)$:

$$(\mathcal{L}_\Theta F)(t) := \bigcap_{l \in S_{n-1}} \left\{ x \in \mathbb{R}^n \mid \langle l, x \rangle \leq (\mathcal{K}_\Theta \delta^l)(t) \right\}. \tag{44}$$

Notice that $\mathcal{L}_\Theta F$ may result in an empty set for some t; in fact, $l \mapsto \mathcal{K}_\Theta \delta^l(t)$ might not be convex and thus, may not be a support function of $(\mathcal{L}_\Theta F)(t)$.

Before discussing the connection to the approach with the directed sets, we notice that Proposition 6 holds true in particular for the embedding of any convex-valued map $F : I \Rightarrow \mathbb{R}^n$ which is sufficiently smooth (in the directed sense). The specialisation to this case yields as one component the (Kergin) interpolation of the support function as in [26], but takes into account also lower-dimensional projections of support faces.

Corollary 3. *Consider Θ on I and μ as in Proposition 6. Let $F : I \Rightarrow \mathbb{R}^n$ be a convex-valued function and $\overrightarrow{F}$ denote its embedding. If F is assumed $(\mu - 1)$-times directed differentiable, then the (Kergin) interpolating map equals*

$$\mathcal{K}_\Theta \overrightarrow{F} = \left(\mathcal{K}_\Theta \overrightarrow{F}^l{}_{n-1}, \mathcal{K}_\Theta \delta^*(l, F(\cdot)) \right)_{l \in S_{n-1}} \tag{45}$$

with $\overrightarrow{F}^l{}_{n-1}(t) = J_{n-1}\left(\Pi^l_{\delta^*(\cdot, F(t))}(Y(l, F(t))) \right)$.

We underline the fact that the second component $\mathcal{K}_\Theta \delta^l(\cdot)$ in (45) coincides with the Newton form of the interpolating polynomial to $\delta^l(\cdot)$ with nodes Θ.

As a consequence of (13) and Remark 1, the visualisation of the interpolation by directed sets actually yields a "super-map" of the approach as in [26], since

$$(\mathcal{K}_\Theta \delta^l)(t) = \sum_{j : \ell_j(t) \geq 0} \ell_j(t) \delta^l(\theta_j) - \sum_{j : \ell_j(t) < 0} |\ell_j(t)| \cdot \delta^l(\theta_j)$$

is the second component of $\mathcal{K}_\Theta \overrightarrow{F}$. It determines the convex part by (9).

Proposition 8. *Let $F : I \Rightarrow \mathbb{R}^n$ be a convex-valued function and assume that all conditions in Corollary 3 hold. Then, it holds for every $t \in I$:*

$$(\mathcal{L}_\Theta F)(t) = P_n((\mathcal{K}_\Theta \overrightarrow{F})(t)) \subseteq V_n((\mathcal{K}_\Theta \overrightarrow{F})(t)) \neq \emptyset. \tag{46}$$

Since the convex part of a directed set may be empty, conditions on the set-valued map F are required in [26, Corollary 2.5] to achieve non-emptiness of the images of the interpolating map $\mathcal{L}_\Theta F$. The following proposition recalls both these conditions and [26, Lemma 2.6].

Proposition 9. *Let $\Theta = (\theta_0, \ldots, \theta_k)$ be a k-grid on I consisting of distinct points and $F : I \rightrightarrows \mathbb{R}^n$ be a convex-valued map. For $t \in I$, set*

$$\varepsilon(t) := \sup_{l \in S_{n-1}} |\delta^l(t) - (\mathcal{K}_\Theta \delta^l)(t)|, \qquad c(t) := \max_{l \in S_{n-1}} (\mathcal{K}_\Theta \delta^l)(t).$$

Then, the following error estimates hold for the two possible cases below:

(i) *If $\delta^*(l, (\mathcal{L}_\Theta F)(t)) = K_\Theta \delta^l(t)$, then*

$$\mathrm{d_H}(F(t), (\mathcal{L}_\Theta F)(t)) = \varepsilon(t).$$

(ii) *Otherwise, if $\delta^*(l, (\mathcal{L}_\Theta F)(t)) < K_\Theta \delta^l(t)$, then we assume additionally the existence of a ball $B_{r(t)}(m(t))$ with centre $m(t) \in \mathbb{R}^n$ and radius $r(t) > 0$ that is a subset of the image $F(t)$ as well as that the error fulfils $0 < \varepsilon(t) < r(t)$. Then,*

$$\mathrm{d_H}(F(t), (\mathcal{L}_\Theta F)(t)) \le \frac{2c(t)}{r(t) - \varepsilon(t)} \cdot \varepsilon(t).$$

Because of the conditions expressed above, the difference of the two support functions of $F(t)$ respectively of $(\mathcal{L}_\Theta F)(t)$ can be estimated through means of the difference $\delta^l(t) - (\mathcal{K}_\Theta \delta^l)(t)$; it also tells us that $(\mathcal{L}_\Theta F)(t)$ is non-empty.

We notice that in [26] the support function $\delta^*(l, F(\cdot))$ of each image $F(t) \in \mathcal{C}(\mathbb{R}^n)$ is interpolated polynomially. Nevertheless, the interpolating map as a whole is not, in general, polynomial as a set-valued function (with respect to the parameter t) like in the approach with directed sets. In the latter approach, the first component leading back to the supporting face is considered, in view of Corollary 3, and interpolated as well. Since $\overrightarrow{\mathcal{D}}^n$ is a Banach space (which also offers a visualisation for all directed sets), the values of the interpolating function $(\mathcal{K}_\Theta \overrightarrow{F})(t)$ always have a non-empty visualisation, see Remark 1. Therefore, an interior ball condition, as in (ii) of the above proposition, is not necessary.

Remark 2. Piecewise constant and linear set-valued interpolation (cf. [41,1,31,29]) are special cases of the Kergin interpolation with directed sets as introduced in Section 4. For the embedded function $\overrightarrow{F}(t) = J_n(F(t))$ and a k-grid Θ with $k \le 1$ different points, it follows that:

$$(\mathcal{K}_\Theta \overrightarrow{F})(t) = \overrightarrow{F}(\theta_0) \quad \text{resp. } (\mathcal{K}_\Theta \overrightarrow{F})(t) = \overrightarrow{F}(\theta_0) + \frac{t - \theta_0}{\theta_1 - \theta_0} \cdot (\overrightarrow{F}(\theta_1) - \overrightarrow{F}(\theta_0)).$$

In both cases, the interpolation of $\overrightarrow{F}(\cdot)$ yields a convex combination of embedded function values. Thus, it coincides with the usual set-valued interpolation

$$V_n((\mathcal{K}_\Theta \overrightarrow{F})(t)) = (\mathcal{L}_\Theta F)(t) = \begin{cases} F(\theta_0) & \text{if } k = 0, \\ \dfrac{\theta_1 - t}{\theta_1 - \theta_0} \cdot F(\theta_0) + \dfrac{t - \theta_0}{\theta_1 - \theta_0} \cdot F(\theta_1) & \text{if } k = 1, \end{cases}$$

by Remark 1. Clearly, $(\mathcal{K}_\Theta \delta^l)(t)$ is the support function of $(\mathcal{L}_\Theta F)(t)$ in both cases.

The error estimates derived in Section 4 are formulated in the Banach space $\overrightarrow{\mathcal{D}}^n$ of directed sets. The following remarks indicate how they can be reinterpreted in the original space

$\mathcal{C}(\mathbb{R}^n)$ of convex, compact sets; a complete answer is challenging and an ongoing subject of research.

Let us consider the special case in which the Hermite interpolation of $\overrightarrow{F}(t) = J_n(F(t))$ delivers an embedded convex set $\overrightarrow{H}(t) = J_n(H(t))$ (as in all examples from Section 6). The metric

$$\mathrm{d_V}(A, B) = \|J_n(A) - J_n(B)\| \quad (A, B \in \mathcal{C}(\mathbb{R}^n))$$

introduced in [2] is equivalent to the Demyanov metric $\mathrm{d_D}(\cdot, \cdot)$; it is stronger than the Hausdorff metric (cf. the discussion in [2]). The estimate

$$\mathrm{d_H}(F(t), H(t)) \le \mathrm{d_V}(F(t), H(t)) = \|J_n(F(t)) - J_n(H(t))\| \tag{47}$$

follows easily. Remark 1 delivers the main argument, since the visualisation of the embedded set $H(t)$ coincides with itself and

$$\mathrm{d_H}(V_n(\overrightarrow{F}(t)), V_n(\overrightarrow{H}(t))) = \mathrm{d_H}(F(t), H(t)).$$

Thus, the achieved error estimates expressed by the norm in $\overrightarrow{\mathcal{D}}^n$ are upper bounds for the "visual distance" of both functions, i.e. the Hausdorff distance of their visualisations.

For the more general case, let us assume that the j-th derivatives

$$D^j\overrightarrow{F}(t) = J_n(F^{(j,1)}(t)) - J_n(F^{(j,2)}(t)),$$
$$D^j\overrightarrow{H}(t) = J_n(H^{(j,1)}(t)) - J_n(H^{(j,2)}(t))$$

are differences of embedded convex sets, $j = 0, \ldots, k$. From the equivalence relation

$$A + D = B + C \tag{48}$$

for pairs of sets $(A, B), (C, D) \in \mathcal{C}(\mathbb{R}^n) \times \mathcal{C}(\mathbb{R}^n)$ in [32], it follows as before

$$\begin{aligned}&\mathrm{d_H}(F^{(j,1)}(t) + H^{(j,2)}(t), H^{(j,1)}(t) + F^{(j,2)}(t))\\ &\quad \le \|J_n(F^{(j,1)}(t) + H^{(j,2)}(t)) - J_n(H^{(j,1)}(t) + F^{(j,2)}(t))\| = \|D^j\overrightarrow{F}(t) - D^j\overrightarrow{H}(t)\|\end{aligned}$$

by using additionally Proposition 1.

To summarise, the corresponding equivalence relation (48) holds approximately, if we know that the error between $D^j\overrightarrow{F}(t)$ and $D^j\overrightarrow{H}(t)$ is small. For the examples in the next section, the Hermite interpolant will produce embedded convex sets as approximations so that the error estimates of Section 4 carry over to the Hausdorff distance of the convex-valued functions. Nevertheless, the derivatives of these functions are no longer embedded convex sets in general (see Examples 2–4). It is therefore convenient to formulate interpolation estimates in the Banach space $\overrightarrow{\mathcal{D}}^n$ keeping the equivalence relation (48) and the preceding remarks in mind.

6. Numerical tests

The computations presented in this section aim to corroborate the theory shown so far; in particular, the interest is focused on the order of convergence. More detailed examples are given in [6]; for similar computations for polynomial interpolation, refer to [33].

In all the presented examples, the function F is sufficiently often directed differentiable on the interval I; this fact follows from easy calculations of the embedding. Furthermore, in

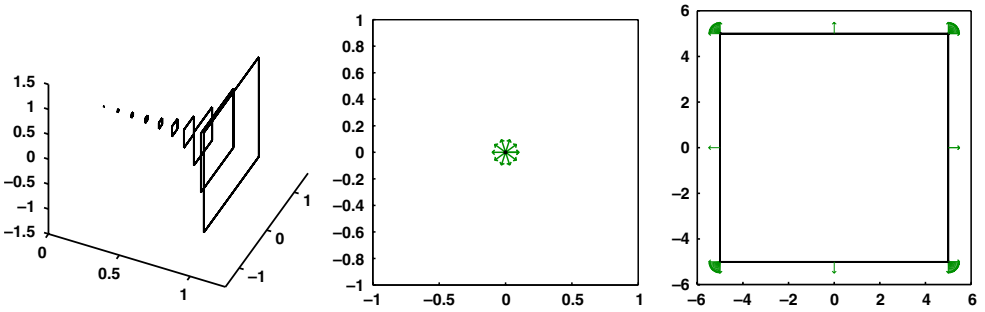

Fig. 1. Funnel of $F(\cdot)$ and derivative data $D\overrightarrow{F}(0)$ and $D\overrightarrow{F}(1)$.

Examples 2–3 the additional geometric conditions of Proposition 9(ii) are satisfied, especially the existence of an interior ball with a uniform radius for all images of the set-valued map F. As Proposition 7 demonstrates and Example 1 shows *inter alia*, no particular geometrical conditions on F have to be assumed for guaranteeing the order of convergence, since the visualisation is always non-empty for directed sets (cf. Proposition 8).

The computations are performed taking into account a discrete set of directions. The perturbation analysis with respect to the finite number of unit directions is discussed in [33, Section 6.1]. The analysis relies on the equivalence between the norm in the space of directed sets and the Demyanov distance, cf. [2].

In Examples 1–3, the derivative at the boundary points are shown. We shall notice that the interpolating map actually matches F within plot precision.

Example 1. We interpolate the set-valued map $F : [0, 1] \Longrightarrow \mathbb{R}^2$ given by $F(t) = t^5 \cdot [-1, 1]^2$. The unit square is scaled by a function with non-negative derivative, cf. left picture in Fig. 1. Hence, $\mathrm{D}\overrightarrow{F}(t) = 5 \cdot t^4 \cdot J_2([-1, 1]^2)$; the values of the derivative consist of embedded convex sets with outer normals, cf. the middle respectively the right picture in the same picture. Incidentally, notice that F violates the geometrical condition mentioned above, since there is no interior of $F(t)$ at time $t = 0$.

For the Hermite interpolation nodes $\Theta = (0, 1), \mu_i = 2, i = 0, 1$, and the test points $\tau_i = \frac{i}{10}$, $i = 0, \ldots, 10$, we get the following error estimate for the Hermite interpolation polynomial $\overrightarrow{H_3}(\cdot)$ of degree 3:

$$\max_{i=0,\ldots,10} \| \overrightarrow{F}(\tau_i) - \overrightarrow{H_3}(\tau_i) \| = 0.0489.$$

Example 2. The convex-valued function F (with its funnel and two derivative values depicted in Fig. 2) to be interpolated reads:

$$F : [0, 1] \Longrightarrow \mathbb{R}^2 : t \mapsto \mathrm{e}^t \cdot [-1, 1]^2 + \frac{1}{2}\mathrm{e}^{-t} \cdot B_1(0). \tag{49}$$

The derivative for the embedded function is a difference of embedded convex sets. The visualisation of the derivative contains a growing convex part and a shrinking non-convex mixed-type part for larger times t.

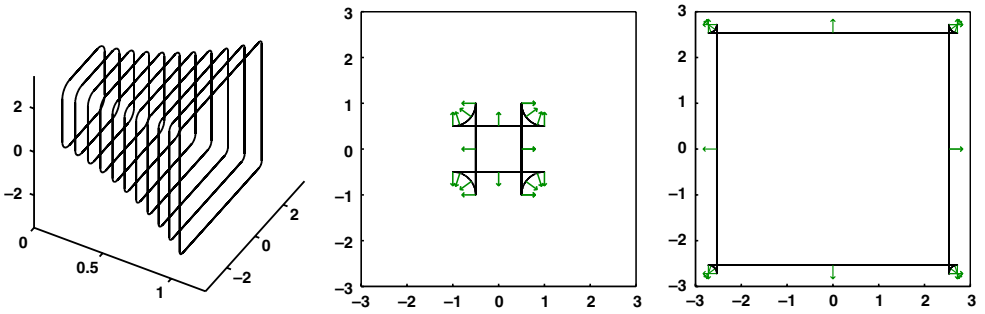

Fig. 2. Funnel of $F(\cdot)$ and derivative data $D\overrightarrow{F}(0)$ and $D\overrightarrow{F}(1)$.

Table 1
Maximal error on test points for piecewise Hermite interpolation.

Number of subintervals N_k	Maximal error ε_k
1	6.982005e−03
2	5.280388e−04
4	3.666896e−05
8	2.421134e−06
16	1.556075e−07
32	9.863408e−09

$$\overrightarrow{F}(t) = \mathrm{e}^t \cdot J_2([-1,1]^2) + \frac{1}{2}\mathrm{e}^{-t} \cdot J_2(B_1(0)),$$
$$D\overrightarrow{F}(t) = \mathrm{e}^t \cdot J_2([-1,1]^2) - \frac{1}{2}\mathrm{e}^{-t} \cdot J_2(B_1(0)).$$

Let us apply the Hermite interpolation piecewise on subintervals $I_i = [\widehat{\theta}_i, \widehat{\theta}_{i+1}]$, where $\widehat{\theta}_i = \frac{i}{N_k}$ with $i = 0, 1, \ldots, N_k = 2^k$, multiplicities $\mu_i = 2$, $i = 0, 1$, and $k = 0, 1, \ldots, 5$. We shall test the theoretical result of Corollary 2. To this end, test points $\tau_j = \frac{j}{M}$, $j = 0, 1, \ldots, M$, with $M = 10 \cdot 2^5 = 320$ are used to evaluate the error

$$\varepsilon_k = \max_{j=0,\ldots,M} \|\overrightarrow{F}(\tau_j) - \overrightarrow{H_3}(\tau_j)\|$$

obtaining the results as in Table 1.

The least square approximation of the logarithmic error bound $\log(C \cdot h^p)$ in Table 1 with the unknown parameters $\log(C)$ and p yields the values $C = 1.007620$ and $p = 3.893485$. This last value is very close to the expected (theoretical) value 4.0.

We highlight that in Examples 1 and 2 the inclusion $F(t_1) \subseteq F(t_2)$ holds for $t_1 \leq t_2$ so that the convex part appears in the visualisation of the derivative.

Example 3 (*Cf. [33, Section 6.2.2]*)**.** In the following example a rotating ellipsoid $\mathcal{E}$ is considered. We set $I = [0, 1]$, $c = (0, 0)$,

$$Q = \begin{pmatrix} 4 & 0 \\ 0 & 1 \end{pmatrix} \quad \text{and, finally,} \quad R(t) = \begin{pmatrix} \cos\left(\frac{\pi}{2}\cdot t\right) & -\sin\left(\frac{\pi}{2}\cdot t\right) \\ \sin\left(\frac{\pi}{2}\cdot t\right) & \cos\left(\frac{\pi}{2}\cdot t\right) \end{pmatrix}.$$

The function then reads

$$F(t) = R(t)\cdot\mathcal{E}(c, Q), \qquad \mathcal{E}(c, Q) = \{x \in \mathbb{R}^2 : \langle x, Q^{-1}x\rangle \le 1\}$$

and its embedding equals $\overrightarrow{F}(t) = J_2(R(t)\cdot\mathcal{E}(c, Q))$.

The images of the set-valued map are strongly convex which results in a smooth case. Although the derivative has an empty convex and concave visualisation part, cf. Fig. 3, its interpolant still has only convex images (which are no longer ellipsoids).

The Hermite interpolating polynomial is computed around the point 0.5 for shrinking intervals $I_k = \left[\frac{1}{2} - \frac{h_k}{2}, \frac{1}{2} + \frac{h_k}{2}\right]$, $h_k = 10^{-k}$, $k = 0, 1, 2, 3$, obtaining the results presented in Table 2. Clearly, the theoretical expected order of convergence 4 is achieved. The least square approximation of the logarithmic error bound $\log(C\cdot h^p)$ in Table 2 yields the values $C = 2.499332$ and $p = 3.790366$. This value for p is close to the expected (theoretical) value 4.0; the first value for ε_0 in Table 2 is a rather good starting value for the error and slightly disturbs the gain of 4 digits after each step.

The interpolation (boundary part with attached normals) achieves a good approximation of the original function, as Fig. 4 exemplifies.

Table 2
Maximal error for the Hermite interpolation at $\tau = 0.5$.

Interval I_k for interpolation	Maximal error ε_k
[0.0, 1.0]	5.740347e−01
[0.45, 0.55]	2.754315e−04
[0.495, 0.505]	2.838795e−08
[0.4995, 0.5005]	2.840173e−12

Example 4. An expanding ball moving along a curve $c(t) = (x(t), y(t))$ for $t \in I = [0, t_0]$ with $t_0 = \sqrt[4]{3}$ originates the convex-valued map:

$$F : [0, \sqrt[4]{3}] \Longrightarrow \mathbb{R}^2 : t \mapsto B_{r(t)}(c(t)), \tag{50}$$

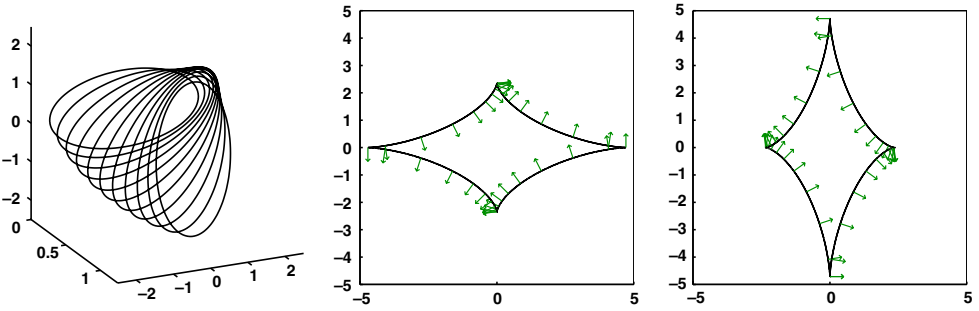

Fig. 3. Funnel of $F(\cdot)$ and derivative data $D\overrightarrow{F}(0)$ and $D\overrightarrow{F}(1)$.

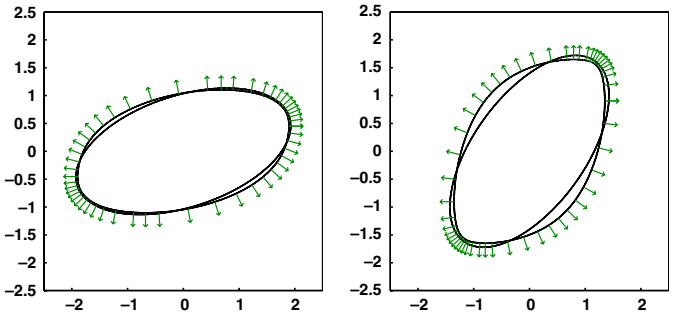

Fig. 4. Comparison of the intermediate values $F(\tau)$ and $\overrightarrow{H_3}(\tau)$ for $\tau = 0.2$ resp. $\tau = 0.6$.

where $r(t) = \frac{1}{4}(\cos(\pi(t+t_0)/t_0)+1)$, $x(t) = t^4 - 1$ and $y(t) = t^5 - t$. We notice straight away that this is a smooth example by rewriting it as a sum of a scaled ball and a vector:

$$F(t) = r(t)B_1(0) + c(t) \tag{51}$$

which allows us to directly obtain the expression for its embedding and its directed derivative

$$\overrightarrow{F}(t) = r(t) \cdot J_2(B_1(0)) + J_2(\{c(t)\}), \tag{52}$$

since the radius $r(t) \geq 0$. The derivative equals

$$D^\mu \overrightarrow{F}(t) = D^\mu r(t) \cdot J_2(B_1(0)) + J_2(\{D^\mu c(t)\}) \tag{53}$$

and is either an embedded ball or its inverse, depending on the sign of $D^\mu r(t)$.

The error estimate on a test-grid $\tau_i := \frac{i}{10} \cdot t_0$ for $i = 0, 1, \ldots, 10$ delivers:

$$\varepsilon = \max_{i=0,\ldots,10} \| \overrightarrow{F}(\tau_i) - \overrightarrow{H_3}(\tau_i) \| = 0.6447253. \tag{54}$$

This is a rather good accuracy, since the Hermite interpolating polynomial has only polynomial degree 3 and the enlargement of the sets as well as the 2D-movement of $\overrightarrow{F}(\cdot)$ in the phase space changes rapidly, cf. Fig. 6.

In Figs. 5 and 6, the linear, quadratic and Hermite interpolation of degree 3 are compared with the original function. In the left column, the 2D-movement in the phase space can be seen, whereas in the right column the t–y-projection of the interpolation polynomial is shown.

For this example, the error $\varepsilon = \max_{i=0,\ldots,10} \| \overrightarrow{F}(\tau_i) - \overrightarrow{H}_3(\tau_i) \|$ is calculated on the test-grid for the various interpolation polynomials. The results are gathered in Table 3 and Figs. 5 and 6. The best result is obtained by the Hermite interpolation.

Table 3
Maximal error on test points for various interpolation polynomials.

Type of interpolation	Maximal error ε
Linear	2.559469
Quadratic	0.808878
Hermite	0.644725

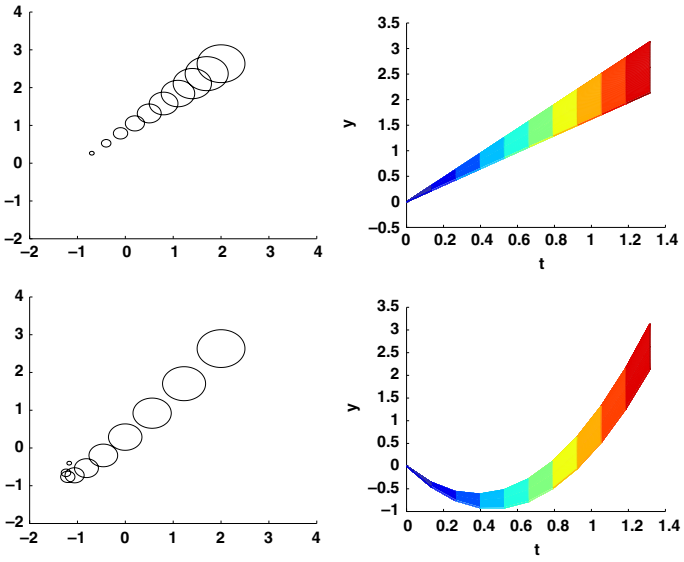

Fig. 5. The linear (first row) and quadratic interpolation for Example 4.

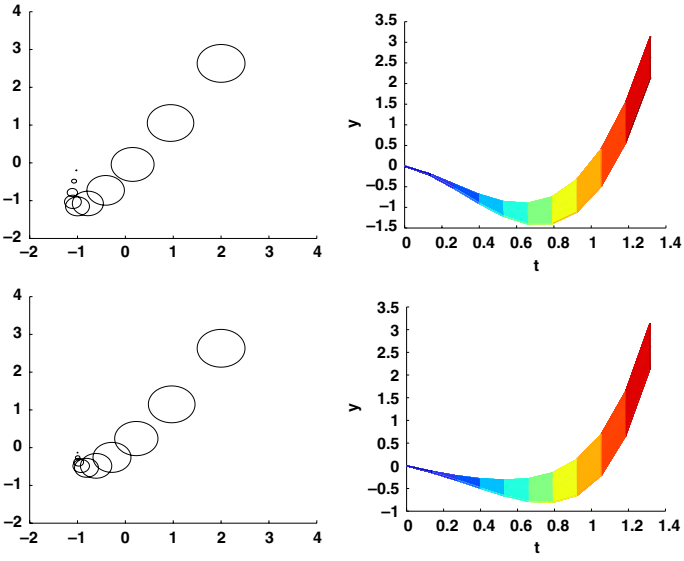

Fig. 6. Hermite interpolation (first row) and original map for Example 4.

7. Conclusions

The Hermite interpolation of set-valued maps with the aid of directed sets produces, as shown in the examples, satisfactory approximations to the original map. The derivatives and the interpolating polynomials, even when involving differences of embedded convex sets or their limits, deliver very reasonable results. Although in the examples the derivative data at the left and right end-points may be inverse to embedded convex sets or even have non-convex visualisation

parts, the Hermite interpolating polynomial has as values always embedded convex images. These facts are by no means to be expected in the general case; the examples are, actually, chosen to demonstrate the potentiality of the approach with directed sets. A first reinterpretation of the error estimates for directed sets within the original space of convex compact sets is presented and relates the Hausdorff distance of the visualisations with the interpolation error in this Banach space. For the simple case of constant and linear interpolation, the presented method coincides with the usual set-valued interpolation, whereas for higher polynomial degree it contains the interpolation based on support functions and on the geometric difference. In contrast to the latter approach, the images of the (directed) interpolating polynomial are always non-empty. In any case, the software used for the calculations also works if the interpolant has non-convex visualisation parts.

Besides the visualisation, another advantage is represented by the space of directed sets itself; it is a Banach space based on a recursive principle and hence it is straight forward to carry over theoretical results from real-valued functions to the set-valued case, as for error estimates on the derivatives of the function and of its interpolant as well as for piecewise interpolation.

Acknowledgments

The authors would like to thank the reviewers for their helpful remarks and Frank Lempio for his continuous support throughout the years.

References

[1] Z. Artstein, Piecewise linear approximation of set-valued maps, J. Approx. Theory 56 (1) (1989) 41–47.
[2] R. Baier, E. Farkhi, Differences of convex compact sets in the space of directed sets, part I: the space of directed sets, Set-Valued Anal. 9 (3) (2001) 217–245.
[3] R. Baier, E. Farkhi, Differences of convex compact sets in the space of directed sets, part II: visualization of directed sets, Set-Valued Anal. 9 (3) (2001) 247–272.
[4] R. Baier, E. Farkhi, Directed derivatives of convex compact-valued mappings, in: N. Hadjisavvas, P.M. Pardalos (Eds.), Advances in Convex Analysis and Global Optimization: Honoring the Memory of C. Caratheodory (1873–1950), in: Nonconvex Optimization and its Applications, vol. 54, Kluwer, Dordrecht, 2001, pp. 501–514.
[5] R. Baier, F. Lempio, Computing Aumann's integral, in: A.B. Kurzhanski, V.M. Veliov (Eds.), Modeling Techniques for Uncertain Systems, Proceedings of a Conference Held in Sopron, Hungary, July 6–10, 1992, in: Progress in Systems and Control Theory, vol. 18, Birkhäuser, Basel, 1994, pp. 71–92.
[6] R. Baier, G. Perria, Hermite interpolation with directed sets, 2008, Preprint, 35 pp. HIM Bonn, http://www.hausdorff-research-institute.uni-bonn.de/preprints.
[7] G. Birkhoff, M.H. Schultz, R.S. Varga, Piecewise Hermite interpolation in one and two variables with applications to partial differential equations, Numer. Math. 11 (3) (1968) 232–256.
[8] S. Bochner, Integration von Funktionen, deren Werte die Elemente eines Vektorraumes sind, Fund. Math. XX (1933) 262–276.
[9] P.J. Davis, Interpolation and Approximation, Dover Publications Inc., New York, 1975.
[10] C. de Boor, A Practical Guide to Splines, Revised ed., in: Applied Mathematical Sciences, vol. 27, Springer-Verlag, New York, 2001, Original published in 1978.
[11] V.F. Demyanov, A. Rubinov, Constructive Nonsmooth Analysis, in: Approximation & Optimization, vol. 7, Peter Lang, Frankfurt am Main, 1995, Russian original "Foundations of nonsmooth analysis, and quasidifferential calculus", Nauka, Moscow, 1990.
[12] P. Deuflhard, A. Hohmann, Numerical Analysis in Modern Scientific Computing. An introduction, 2nd ed., in: Texts in Applied Mathematics, vol. 43, Springer, New York, Berlin, Heidelberg, 2003, First edition published in 1995.
[13] P. Diamond, P. Kloeden, A. Rubinov, A. Vladimirov, Comparative properties of three metrics in the space of compact convex sets, Set-Valued Anal. 5 (3) (1997) 267–289.
[14] T.D. Donchev, E. Farkhi, Moduli of smoothness of vector valued functions of a real variable and applications, Numer. Funct. Anal. Optim. 11 (5–6) (1990) 497–509.

[15] A.L. Dontchev, F. Lempio, Difference methods for differential inclusions: a survey, SIAM Rev. 34 (2) (1992) 263–294.
[16] N. Dyn, D. Levin, Analysis of Hermite-type subdivision schemes, in: C.K. Chui, L.L. Schumaker (Eds.), Approximation Theory VIII. Vol. 2. Wavelets and Multilevel Approximation. Proc. of the 8th Texas Internat. Conf. Held at Texas A & M Univ., College Station, TX, January 8–12, 1995, in: Ser. Approx. Decompos., vol. 6, World Scientific Publishing Co., Inc., River Edge, NJ, 1995, pp. 117–124.
[17] L. Filipsson, Kergin interpolation in Banach spaces, J. Approx. Theory 127 (1) (2004) 108–123.
[18] M. Gasca, T. Sauer, Polynomial interpolation in several variables. Multivariate polynomial interpolation, Adv. Comput. Math. 12 (4) (2000) 377–410.
[19] H.S. Goghary, S. Abbasbandy, Interpolation of fuzzy data by Hermite polynomial, Int. J. Comput. Math. 82 (5) (2005) 595–600.
[20] R.E. Grundy, The application of Hermite interpolation to the analysis of non-linear diffusive initial-boundary value problems, IMA J. Appl. Math. 70 (6) (2005) 814–838.
[21] H. Hadwiger, Minkowskische Addition und Subtraktion beliebiger Punktmengen und die Theoreme von Erhard Schmidt, Math. Z. 53 (3) (1950) 210–218.
[22] K. Hormann, S. Spinello, P. Schröder, C^1-continuous terrain reconstruction from sparse contours, in: T. Ertl, B. Girod, G. Greiner, H. Niemann, H.-P. Seidel, E. Steinbach, R. Westermann (Eds.), Proc. 8th Int. Worksh. Vision, Modeling, and Visualization, IOS Press, 2003, pp. 289–297.
[23] K. Kansy, Elementare Fehlerdarstellung für Ableitungen bei der Hermite-Interpolation, Numer. Math. 21 (4) (1973–74) 350–354.
[24] E. Kaucher, Interval analysis in the extended interval space $\mathbb{IR}$, Comput. Suppl. 2 (1980) 33–49.
[25] P. Kergin, A natural interpolation of C^k functions, J. Approx. Theory 29 (4) (1980) 278–293.
[26] F. Lempio, Set-valued interpolation, differential inclusions, and sensitivity in optimization, in: R. Lucchetti, J. Revalski (Eds.), Recent Developments in Well-Posed Variational Problems, in: Mathematics and its Applications, vol. 331, Kluwer, Dordrecht, 1995, pp. 137–169.
[27] A. Lin, M. Walker, Proto-Bézier simplices—applications to Hermite interpolation of curves, in: Geometric Modeling and Computing: Seattle 2003, in: Mod. Methods Math., Nashboro Press, Brentwood, TN, 2004, pp. 387–404.
[28] C. Manni, On shape preserving C^2 Hermite interpolation, BIT 41 (1) (2001) 127–148.
[29] S.M. Markov, E. Popova, U. Schneider, J. Schulze, On linear interpolation under interval data, Math. Comput. Simulation 42 (1) (1996) 35–45.
[30] Ch.A. Micchelli, A constructive approach to Kergin interpolation in $\mathbb{R}^k$: multivariate B-splines and Lagrange interpolation, Rocky Mountain J. Math. 10 (1980) 485–497.
[31] M.S. Nikol'skiĭ, Local approximation of first order to set-valued mappings, in: A.B. Kurzhanski, V.M. Veliov (Eds.), Set-valued Analysis and Differential Inclusions. A Collection of Papers resulting from a Workshop held in Pamporovo, Bulgaria, September, 1990, in: Progress in Systems and Control Theory, vol. 16, Birkhäuser, Boston, MA, 1993, pp. 149–156.
[32] D. Pallaschke, R. Urbański, Pairs of Compact Convex Sets. Fractional Arithmetic with Convex Sets, in: Mathematics and its Applications, vol. 548, Kluwer, Dordrecht, 2002.
[33] G. Perria, Set-valued interpolation, Bayreuth. Math. Schr. 79 (2007) 154 pp.
[34] H. Petersson, Kergin interpolation in Banach spaces, Studia Math. 153 (2) (2002) 101–114.
[35] H. Prautzsch, W. Böhm, M. Palunszny, Bézier and B-Spline Techniques, in: Mathematics and Visualization, Springer, Berlin, 2002.
[36] P.M. Prenter, Lagrange and Hermite interpolation in Banach spaces, J. Approx. Theory 4 (4) (1971) 419–432.
[37] R.T. Rockafeller, Convex Analysis, 2nd ed., in: Princeton Mathematical Series, vol. 28, Princeton University Press, Princeton, NJ, 1972, first edition in 1970.
[38] R. Schneider, Convex Bodies: The Brunn-Minkowski Theory, in: Encyclopedia of Mathematics and its Applications, vol. 44, Cambridge University Press, Cambridge, 1993.
[39] S. Simon, Kergin approximation in Banach spaces, J. Approx. Theory 154 (2) (2008) 181–186.
[40] J. Stoer, R. Bulirsch, Introduction to Numerical Analysis, 3rd ed., in: Texts in Applied Mathematics, vol. 12, Springer, New York, NY, 2002, Transl. from the German by R. Bartels, W. Gautschi, and C. Witzgall.
[41] R.A. Vitale, Approximation of convex set-valued functions, J. Approx. Theory 26 (4) (1979) 301–316.